

Impurities and Nuclear Spin Relaxation in Aluminum

L. C. HEBEL, JR.

Bell Telephone Laboratories, Murray Hill, New Jersey

(Received May 8, 1962)

Both positive- and negative-temperature nuclear spin distributions are used to study the nuclear spin-lattice relaxation in zero external field at liquid helium temperatures in aluminum with controlled impurity content. The relaxation shows considerable deviation from previous theoretical predictions, which were based on the assumption of a single nuclear spin temperature. Most of the deviation is removed by introducing strong impurity effects at zero field, which result in cross relaxation within the nuclear spin system. In addition, the magnetic-field dependence of the relaxation is measured, and the results are compared to theoretical predictions.

I. INTRODUCTION

IN metals at low temperatures, nuclear spins come into thermal equilibrium with their surroundings by means of energy exchanges (collisions) with the conduction electrons; this process, called "nuclear spin-lattice relaxation," results from the hyperfine interaction between the magnetic moments of the conduction electrons and those of the nuclei.¹ In an external magnetic field, nuclear spin-lattice relaxation is often described as the growth or decay of the bulk nuclear magnetization, M , towards its thermal equilibrium value, M_0 , given by Curie's law:

$$M_0 = CH_0/T, \quad (1)$$

where C is the nuclear Curie constant, H_0 is the external field, and T is the lattice temperature. The process of growth or decay is usually exponential with a time constant \mathcal{T}_1 , the nuclear spin-lattice relaxation time. The magnetization is a convenient variable to use since it can be measured directly by the amplitude of a nuclear resonance signal.

As an alternative description, the nuclear spins are regarded as a system that is characterized by a spin temperature, T_s .² That is, if p_n and p_m are the populations of the n th and m th nuclear spin levels with energies E_n and E_m , then

$$p_n/p_m = \exp[(E_m - E_n)/kT_s]. \quad (2)$$

Such a distribution leads to a Curie-like law for the magnetization.

$$M = CH_0/T_s. \quad (3)$$

Spin-lattice relaxation is regarded as a change in spin temperature as the nuclei come into thermal equilibrium with their surroundings. In strong external fields the two treatments are equivalent and are characterized by the same \mathcal{T}_1 .

The magnetic-field dependence of \mathcal{T}_1 in metals at low external fields was investigated by Redfield³ and by Hebel and Slichter⁴ in conjunction with studies of \mathcal{T}_1 in

normal and superconducting aluminum. Anderson and Redfield⁵ also have reported extensive measurements of \mathcal{T}_1 vs external field in lithium, sodium, and copper and have noted some deviations from theoretical predictions.

This paper is primarily concerned with measurements and interpretation of relaxation in aluminum at zero external magnetic field in the presence of impurities. The dynamics of an isolated nuclear spin system at zero field has been discussed in detail by Abragam and Proctor⁶ and by Hebel and Slichter.⁴ Curie's law shows that, independent of T_s , there is no bulk nuclear magnetization at zero field (provided there is no nuclear ferromagnetism). Thus, zero-field relaxation cannot be described by changes in bulk magnetization. Of course, there is order in the nuclear spin system even at zero external field; that is, there exists preferential alignment of spins in the local field of neighboring spins. An exact calculation of zero-field relaxation would require a solution of the problem of many nuclear spins coupled together by their dipolar fields; as yet no such solution has been obtained. Consequently, since the bulk magnetization approach is useless and since an exact theory of \mathcal{T}_1 at zero field does not exist, the *assumption* has been made previously that the nuclear spin system at zero field is characterized by a spin temperature even while the system is relaxing. With the aid of the spin-temperature assumption the calculation of \mathcal{T}_1 at zero field can be carried through completely.^{3,4}

The experiments on aluminum which are presented use both positive- and negative-temperature initial-spin distributions to test the above assumption. The results show considerable deviation from previous theoretical predictions based on the assumption of a single nuclear spin temperature, especially for samples of controlled impurity content. Most of the discrepancy between theory and experiment can be removed by introducing strong impurity effects which result in cross relaxation within the nuclear spin system at zero field. In Sec. II the method of measurement and the experimental details are given. In Sec. III the relevant interactions are presented and calculations of zero-field relaxation

¹ See, for example, D. F. Holcomb and R. E. Norberg, *Phys. Rev.* **98**, 1074 (1955). For aluminum, see J. J. Spokas and C. P. Slichter, *ibid.* **113**, 1462 (1959).

² H. G. B. Casimir and F. K. du Pré, *Physica* **5**, 507 (1938).

³ A. G. Redfield, *IBM J. Research Develop.* **1**, 19 (1957).

⁴ L. C. Hebel and C. P. Slichter, *Phys. Rev.* **113**, 1504 (1959).

⁵ A. G. Anderson and A. G. Redfield, *Phys. Rev.* **116**, 583 (1959).

⁶ A. Abragam and W. G. Proctor, *Phys. Rev.* **109**, 1441 (1958).

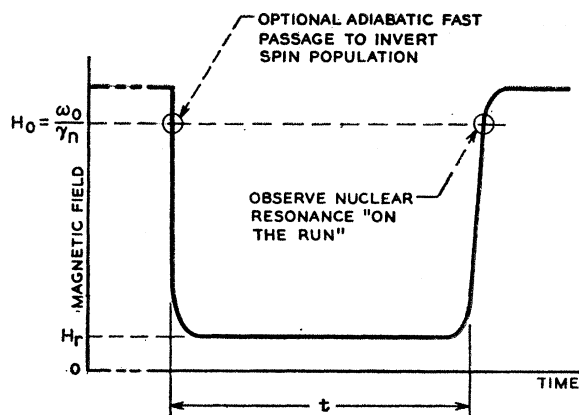


FIG. 1. Schematic plot of external magnetic field, H_0 , vs time, t .

are made. The data are presented in Sec. IV, and finally, conclusions follow in Sec. V.

II. MEASUREMENT AND EXPERIMENTAL DETAILS

Zero-field relaxation was studied by disturbing the nuclear spin system with an external field and observing the recovery to thermal equilibrium; a schematic plot of the external field versus time is shown in Fig. 1. The following cycle will be referred to as the cycle of measurement: the external field was held well above the value for nuclear resonance for a long enough time for the nuclear spins to achieve thermal equilibrium at liquid helium temperatures; the field was then quickly turned to zero, and the nuclear spins were allowed to relax for a time t ; then the field was quickly turned on again, and the nuclear resonance signal was measured on the run as the magnetic field passed through the resonance value.

The field switching must be fast compared to the relaxation times to be measured but slow enough to be reversible, which usually means slow compared to T_2 , the nuclear spin-spin relaxation time. Hebel and Slichter⁴ discuss the requirement in more detail; it is easily satisfied in aluminum at liquid helium temperatures where $T_2 = 40 \mu\text{sec}$ and the relaxation times to be studied are 0.05 to 0.5 sec. In the absence of spin-lattice relaxation, reversible field cycling allows full recovery at the time of measurement of the nuclear magnetization present before the cycle, even though the magnetization was zero during the time t at zero field. Since the amplitude of the nuclear resonance signal is directly proportional to the nuclear magnetization, study of the nuclear resonance signal versus the time t determines the relaxation that took place at zero field. Relaxation in low magnetic fields could be studied by switching the external field down to some residual value rather than to zero field.

In addition, adiabatic fast passage was used at the beginning of the cycle to obtain inverted spin populations to allow study of zero-field relaxation of systems with negative-temperature spin distributions. Except

for the initial use of adiabatic fast passage, the cycle of measurement is that used by Hebel and Slichter,⁴ and Anderson and Redfield,⁵ and is similar to that used by Sachs and Turner,⁷ Ramsey and Pound,⁸ and Abragam and Proctor.⁶

The nuclear resonance signal was observed with a cross-coil spectrometer. The oscillator and receiver coils were crossed at room temperature with the sample inside them by rotating the receiver coil and were then locked snugly in place. At liquid helium temperatures there was some coupling between coils which was cancelled to any desired degree in the first rf stage, which was a cascode type. The signal was fed onto the lower grid, and a reference signal from the oscillator was fed through a cathode follower onto the upper grid; by varying the phase and amplitude of the reference signal a very quiet and stable balance could be obtained. Unbalanced signal was used after amplification to provide rf phase-sensitive detection, so that either the dispersion or absorption signal could be used. An excellent signal-to-noise ratio was obtained even in the presence of pump vibration because of the stable, adjustable balance.

The external field was provided by two solenoids placed in the liquid nitrogen Dewar. One solenoid was end corrected to give a uniform field of about 500 G at the center and was used to observe the nuclear resonance signal. The second solenoid was designed to give a field of up to 1500 G and was used only during the time that the spins were initially coming into thermal equilibrium. Both solenoids were critically damped and could be cut off in a few milliseconds to begin the cycle of measurement; the end-corrected solenoid could be turned on equally fast to observe the resonant signal at the end of the cycle. The resonant signal was displayed on an oscilloscope and photographed using a polaroid camera; each cycle was repeated several times and the photographs were superimposed on the film to improve the signal-to-noise ratio.

The samples were powdered aluminum sieved through a 400-mesh sieve and were immersed in liquid helium to avoid sample heating effects due to rf and pulsed fields. To demonstrate impurity effects, samples of controlled zinc impurity were made by the following method: A known amount of pure zinc was melted with the zone-refined aluminum, and when cooled, drawn into 55-mil wire; the wire was fed into a metallizing gun which had been carefully cleaned; the metallized spray was collected in pure water and the particles dried and sieved. Analysis showed that samples so produced remained very pure throughout the process, and in excess of 50% passed through the 400-mesh sieve. In one sample the nuclear relaxation was measured before and after annealing, but no difference was observed. The remaining samples were not annealed (except at room temperature) because of the problem of sintering. The

⁷ E. Turner, thesis, Harvard University, 1949 (unpublished).

⁸ N. F. Ramsey and R. V. Pound, *Phys. Rev.* **81**, 278 (1951).

atomic percent of zinc impurity was determined by using quantitative spectrographic analysis to compare some of each sample against samples of known impurity content.

III. IMPURITIES AND ZERO-FIELD RELAXATION

A detailed analysis of the cycle of measurement has been given in reference 4 based on the assumption that the nuclear spin system is characterized by a single spin temperature throughout the cycle. The cycle was treated as an adiabatic demagnetization to a low nuclear spin temperature followed by relaxation of the spin temperature toward the lattice temperature and, finally, completed by an adiabatic remagnetization. The magnetization measured afterwards was shown to relax exponentially with time. That is,

$$M'(t) = (M_0 - M_{\text{loc}}) \exp[-t/T_1(0)] + M_{\text{loc}}, \quad (4)$$

where $M'(t)$ is the magnetization measured using nuclear resonance and $T_1(0)$ is the value of T_1 at zero external field at the lattice temperature. M_{loc} is a small magnetization obtained in a field of order of the local field at the nuclear site due to neighboring nuclei; it reflects the order (preferential alignment) present even at zero field. The calculation can also be carried through for a negative spin temperature at the start of the cycle; one finds the same result as Eq. (4) except M_0 is replaced by $-M_0$. Thus, a semilog plot of $(M' - M_{\text{loc}})$ vs t should give a straight line whose slope is the same for both positive and negative initial spin temperatures.

The external magnetic-field dependence of T_1 furnishes another test of the spin-temperature assumption for nuclear relaxation. In the theory of the field dependence of T_1 the hyperfine interaction is used in a perturbation calculation to transfer energy between the nuclear spin system and the lattice via the conduction electrons. The hyperfine Hamiltonian for "S" electrons may be written as

$$\mathcal{H}' = \frac{8\pi}{3} \gamma_e \gamma_n \hbar^2 \sum_{i,j} \mathbf{I}_i \mathbf{S}_j \delta(\mathbf{R}_i - \mathbf{r}_j), \quad (5)$$

where γ_n and \mathbf{I}_i are the gyromagnetic ratio and spin operator for the i th nucleus at \mathbf{R}_i , γ_e and \mathbf{S}_j are the gyromagnetic ratio and spin operator for the j th electron at \mathbf{r}_j , and $\delta(\mathbf{R}_i - \mathbf{r}_j)$ is a Dirac delta function. In a strong external field the zero-order nuclear spin Hamiltonian is taken as the Zeeman interaction with the external field; the conduction electrons are characterized by Bloch functions and a Fermi distribution at the lattice temperature. One-electron calculations^{9,10} then give

$$\frac{1}{T_1} = \left(\frac{16}{9\pi} \right) \left(\frac{mk_F \gamma_e \gamma_n}{\hbar} \right)^2 V^2 |\psi(0)|^4 kT, \quad (6)$$

where $\psi(0)$ is the wave function evaluated at a nuclear site of a conduction electron of mass m and Fermi wave vector k_F , V is the normalizing volume, and k is the Boltzmann constant. The inverse temperature dependence of T_1 is very characteristic of the conduction electron relaxation process.

For an arbitrary external magnetic field Hebel and Slichter⁴ and Redfield⁸ used the Zeeman interaction plus the nuclear dipole-dipole interaction as the zero-order nuclear spin Hamiltonian. That is, if the external field is denoted by H ,

$$\mathcal{H} = \mathcal{H}_Z + \mathcal{H}_D, \quad (7)$$

where

$$\mathcal{H}_Z = -\gamma_n \hbar H \sum I_{iz}, \quad (8)$$

and

$$\mathcal{H}_D = \frac{1}{2} \sum_{i,j} \frac{\gamma_n^2 \hbar^2}{R_{ij}^3} \left[\mathbf{I}_i \cdot \mathbf{I}_j - \frac{3(\mathbf{I}_i \cdot \mathbf{R}_{ij})(\mathbf{I}_j \cdot \mathbf{R}_{ij})}{R_{ij}^2} \right]. \quad (9)$$

With the aid of the spin temperature assumption a perturbation calculation³⁻⁵ yields

$$T_{1D}(H) = T_1(H^2 + h_D^2)/(H^2 + 2h_D^2), \quad (10)$$

where T_1 is given by Eq. (6); using "tr" for trace,¹¹

$$h_D^2 = H^2 \text{Tr} \mathcal{H}_D^2 / \text{Tr} \mathcal{H}_Z^2 = (5/3) \langle \Delta H^2 \rangle_{\text{av}}. \quad (11)$$

In Eq. (11) $\langle \Delta H^2 \rangle_{\text{av}}$ is the Van Vleck second moment¹² of the nuclear resonance absorption line in a powder, so that h_D^2 is of the order of the mean square local field at a nucleus due to the dipolar field of its neighbors. At zero field,

$$T_{1D}(0) = \frac{1}{2} T_1. \quad (12)$$

Thus, $T_{1D}(0)$ should also be inversely proportional to temperature.

In a preliminary communication¹³ it was pointed out that the above treatment for aluminum could not be correct in the presence of impurities. Aluminum has an electric quadrupole moment which can interact with electric field gradients when impurities break up the cubic symmetry of the aluminum lattice. Such electric field gradients are screened by the conduction electrons; but Friedel¹⁴ and Kohn and Vosko¹⁵ have pointed out that the sharpness of the cutoff of electron momenta at the Fermi momentum results in a strong, long-range, electric field gradient which changes sign periodically as a function of distance from the impurity. The asymptotic electric field gradient, $eq(r)$, is of the form

$$eq(r) = A \cos(2k_F r + \varphi)/r^3, \quad (13)$$

where the amplitude A and the phase φ are determined

¹¹ Equation (11) corrects a factor of 2 error which appears in similar equations in references 3 and 5.

¹² J. H. Van Vleck, Phys. Rev. **74**, 1168 (1948). For experimental values in aluminum, see part 2 of reference 1.

¹³ L. C. Hebel, Bull. Am. Phys. Soc. **5**, 176 (1960).

¹⁴ J. Friedel, Phil. Mag. **43**, 153 (1952); Suppl. Nuovo cimento **2**, 287 (1958); A. Blandin and J. Friedel, J. phys. radium, **21**, 689 (1960).

¹⁵ W. Kohn and S. H. Vosko, Phys. Rev. **119**, 912 (1960).

⁹ J. Korringa, Physica **16**, 601 (1950).

¹⁰ A. W. Overhauser, Phys. Rev. **89**, 689 (1953).

by the particular impurity. Such a gradient gives rise to an additional term in the zero-order nuclear Hamiltonian:

$$\mathcal{H}_Q = \sum_{i,k} \frac{e^2 Q q(R_{ik})}{4I(2I-1)} [3I_z^2 - I(I+1)], \quad (14)$$

where eQ is the quadrupole moment of the i th solute nucleus at a distance \mathbf{R}_{ik} from the k th impurity.

With the aid of the spin-temperature assumption, spin-lattice relaxation can be calculated using \mathcal{H}_Q , Eq. (14), in place of \mathcal{H}_D , Eq. (9), in the zero-order nuclear spin Hamiltonian. Expressions result which are similar to those of Eqs. (10), (11), and (12). Labeling the relaxation time τ_{1Q} to distinguish it from τ_{1D} ,

$$\tau_{1Q}(H) = \tau_1 (H^2 + h_Q^2) / (H^2 + 3h_Q^2); \quad (15a)$$

$$\tau_{1Q}(0) = \frac{1}{3} \tau_1, \quad (15b)$$

where τ_1 is from Eq. (6) and

$$h_Q^2 = H^2 \text{Tr} \mathcal{H}_Q^2 / \text{Tr} \mathcal{H}_D^2. \quad (16)$$

Thus, the form of the field dependence of $\tau_{1Q}(H)$ is similar to that of $\tau_{1D}(H)$, Eq. (10). However, $\tau_{1Q}(0)/\tau_1 = \frac{1}{3}$, whereas $\tau_{1D}(0)/\tau_1 = \frac{1}{2}$; also h_Q^2 could be much larger than $h_D^2 = (5/3) \langle \Delta H^2 \rangle_{av}$.

Kohn and Vosko¹⁵ have calculated the coefficients A and φ of Eq. (13) for several impurities in copper. Rowland¹⁶ has checked the theory by adding impurities to pure copper and measuring the loss of intensity of the copper nuclear resonance due to quadrupolar broadening. From a study of the intensity versus concentration of impurity, he determines n_0 , the number of copper nuclei per impurity for which the nuclear quadrupole interaction with the impurity is greater than the quadrupolar line breadth. Rowland finds that his experimental values of n_0 in copper are large and are in good agreement with the theoretical values of Kohn and Vosko.

No calculations are available for aluminum. However, both Rowland¹⁷ and Weinberg¹⁸ have measured n_0 for zinc impurity in aluminum; Rowland found $n_0 = 98$. Such a large number of nuclei per impurity with a quadrupolar interaction greater than their rms dipolar interaction means that quadrupolar effects must be considered in nuclear zero field relaxation for all ordinary impurity concentrations.

As a result it is convenient to divide the nuclei into two groups to calculate zero-field spin relaxation. Those spins near an impurity have quadrupolar splittings greater than the rms dipolar energy; such spins will be referred to as the “ Q ” spins, and their zero-order Hamiltonian is taken to be \mathcal{H}_Q . In a dilute alloy there are also spins sufficiently far from an impurity to have an rms dipolar energy greater than their quadrupolar

splittings; such spins will be referred to as “ D ” spins, and their zero-order spin Hamiltonian is taken to be \mathcal{H}_D . The spins at the boundary, which are intermediate between “ Q ” and “ D ,” are ignored in first approximation. For both types of spins, \mathcal{H}' is regarded as the perturbation which transfers energy to the lattice via the conduction electrons. Since the field gradient near the impurity is only a function of distance for equivalent direction in a lattice, the Q system is actually made up of subsystems corresponding to the various shells of neighbors near the impurity. For face-centered cubic aluminum the twelve nearest neighbors would form the subsystem with the largest quadrupole splitting, and the splittings for the various shells should scale like $\cos(2\mathbf{k} \cdot \mathbf{r} + \varphi)/r^3$. Within each subsystem, the dipolar interaction can easily cause mutual spin flips since all spins have the same quadrupole splitting. Thus, \mathcal{H}_D must be regarded as an important perturbation which establishes internal equilibrium within each subsystem.

Consequently, in the spin-temperature approximation the D spins are assumed to be characterized by a spin temperature T_{SD} . Also, each shell of the Q system is assumed to be characterized by a spin temperature, T_{SQi} , because of internal spin flips induced by dipolar coupling. In addition, due to dipolar coupling there will be a diffusion of spin energy (thermal mixing) between shells and between Q and D spins as the spins approach thermal equilibrium. Thus, *there must exist a cross-relaxation process internal to the nuclear spin system in addition to the τ_1 process*. A detailed calculation of the cross-relaxation process is not possible without knowledge of the exact quadrupole splittings of the spins in each shell. For typical impurity concentrations a rough estimate using ordinary spin-diffusion theory indicates that the time for diffusion from the Q to the D system should be between several hundred and a thousand times τ_2 , the spin-spin relaxation time. This would be 10 to 30 msec and much shorter than τ_{1D} , which is inversely proportional to temperature and about 400 msec at 1.5°K at zero field in pure samples.

Spin-flip process induced by dipolar coupling will also cause diffusion of spin energy from shell to shell within the Q system. Even though spins in different shells may be near neighbors, the difference in quadrupolar splittings may be much larger than the dipolar splitting; thus spin diffusion from shell to shell should proceed by multiple spin-flip mechanisms of the types invoked by Bloembergen, Shapiro, Pershan, and Artman¹⁹ to account for the spin calorimetry experiments of Abragam and Proctor.⁶ The time constants for diffusion from shell to shell will be assumed to be less than or equal to the above-mentioned time for diffusion between Q and D systems and certainly less than τ_{1Q} or τ_{1D} . Such assumptions are justified by the data *a fortiori* and lead to the following simple picture of zero-field relaxation: The shells of the Q system relax with essentially a single

¹⁵ T. J. Rowland, Phys. Rev. **119**, 900 (1960).

¹⁷ T. J. Rowland, Acta. Met. **3**, 74 (1955).

¹⁸ D. L. Weinberg, J. Phys. Chem. Solids **15**, 249 (1960).

¹⁹ N. Bloembergen, S. Shapiro, P. S. Pershan, and J. O. Artman, Phys. Rev. **114**, 445 (1959).

spin temperature, T_{SQ} ; after the initial adiabatic demagnetization to separate, cold spin temperatures, T_{SQ} and T_{SD} relax toward common spin temperature at zero field with a cross-relaxation time, τ_{12} , which is independent of the lattice temperature and which is much shorter than τ_{1Q} or τ_{1D} ; then the two systems relax together toward the lattice temperature. Since most of the resonance signal results from D spins because of the quadrupolar broadening of the Q spin levels, the zero-field relaxation should display a cross-relaxation "component" whose magnitude relative to the τ_1 "component" should be a strong function of impurity concentration. The situation is similar to the low-field spin relaxation in alkali halides analyzed by Schumacher²⁰ using the method of reference 4. In Appendix I, his equations are applied to the Q and D systems to show that when $\tau_{12} \ll \tau_{1D}(0)$ and $\tau_{1Q}(0)$, the spins indeed have a "two-mode" relaxation, a τ_{12} mode and a mixed τ_1 mode; the system which dominates the τ_1 is that with the greater spin specific heat.

Using the above assumptions, the fraction of τ_{12} mode can be calculated. The field switching-relaxation cycle will be analyzed by extending the method of reference 4 to treat both the Q and D systems. In the cycle both spin systems are first adiabatically demagnetized starting from thermal equilibrium with magnetization, M_0 , in a field, H_0 , at the lattice temperature, T . For an adiabatic process, thermodynamics shows that for each system

$$dQ = 0 = \zeta_H dT_S + T_S (\partial M / \partial T_S)_H dH, \quad (17)$$

where ζ_H is the spin specific heat at constant field and M is the magnetization. M is obtained from the Curie-like law, Eq. (3); ζ_H can be obtained from the spin energy, \bar{E} , by differentiating with respect to T_S at constant field. The spin energies for each system are obtained by evaluating

$$\bar{E} = \{ \text{Tr}[\mathcal{H} \exp(-\mathcal{H}/kT_S)] / \text{Tr}[\exp(-\mathcal{H}/kT_S)] \}.$$

One finds

$$\bar{E}_D = -C_D(H^2 + h_D^2)/T_D, \quad (18a)$$

$$\bar{E}_Q = -C_Q(H^2 + h_Q^2)/T_Q, \quad (18b)$$

where H is the external field, C_D and C_Q are Curie constants, and h_Q and h_D are effective local fields.

$$C_D = \text{Tr}_D \mathcal{H}^2 / \kappa H^2 \text{Tr}_D 1, \quad (19a)$$

$$C_Q = \text{Tr}_Q \mathcal{H}^2 / \kappa H^2 \text{Tr}_Q 1, \quad (19b)$$

$$h_D^2 = H^2 \text{Tr}_D \mathcal{H}^2 / \text{Tr}_D \mathcal{H}^2 \cong (5/3) \langle \Delta H^2 \rangle_{\text{av}}, \quad (19c)$$

$$h_Q^2 = H^2 \text{Tr}_Q \mathcal{H}^2 / \text{Tr}_Q \mathcal{H}^2, \quad (19d)$$

where Tr_D and Tr_Q denote traces over the Q and D spins, respectively.

Using the above equations to obtain the spin specific heats and using Eq. (3) for M , Eq. (17) may be integrated from the initial field, H_0 , to 0. One finds that the

spin systems demagnetize to separate spin temperatures, T_{Q0} and T_{D0} , given by

$$\frac{1}{T_{Q0}} = \frac{1}{T} \left[1 + \left(\frac{H_0}{h_Q} \right)^2 \right]^{\frac{1}{2}} \cong \frac{1}{T} \left(\frac{H_0}{h_Q} \right), \quad (20a)$$

$$\frac{1}{T_{D0}} = \frac{1}{T} \left[1 + \left(\frac{H_0}{h_D} \right)^2 \right]^{\frac{1}{2}} \cong \frac{1}{T} \left(\frac{H_0}{h_D} \right). \quad (20b)$$

To calculate the fraction of τ_{12} mode, τ_1 is set infinite. The spins interact at zero field and come to a common spin temperature, T_{S1} , in a time τ_{12} . Equating energies before and after thermal mixing, using Eq. (18),

$$C_Q h_Q^2 / T_{Q0} + C_D h_D^2 / T_{D0} = (C_Q h_Q^2 + C_D h_D^2) / T_{S1}. \quad (21)$$

Remagnetization to the original field is again described by Eq. (17), this time integrating from 0 to H_0 with the help of Eqs. (3), (18), and (19). The spins remagnetize to spin temperatures $T_{Q'}$ and $T_{D'}$ given by

$$\frac{1}{T_{Q'}} \cong \frac{1}{T_{S1}} \left(\frac{h_Q}{H_0} \right), \quad (22a)$$

$$\frac{1}{T_{D'}} \cong \frac{1}{T_{S1}} \left(\frac{h_D}{H_0} \right). \quad (22b)$$

Substitution of Eqs. (20) and (21) into (22) shows that

$$T / T_{Q'} = (C_Q h_Q^2 + C_D h_D h_Q) / (C_Q h_Q^2 + C_D h_D^2), \quad (23a)$$

$$T / T_{D'} = (C_Q h_Q h_D + C_D h_D^2) / (C_Q h_Q^2 + C_D h_D^2). \quad (23b)$$

Now the $\frac{1}{2} - \frac{1}{2}$ spin transition is not quadrupolar broadened in first order, so that approximately $\frac{1}{4}$ of the Q magnetization contributes to the resonance signal for a spin of $\frac{5}{2}$; thus, the fractional signal remaining after a cycle for pure cross relaxation is given by

$$f = (\frac{1}{4} M_{Q'} + M_{D'}) / M_0 = (\frac{1}{4} C_Q H_0 / T_{Q'} + C_D H_0 / T_{D'}) / (\frac{1}{4} C_Q H_0 / T + C_D H_0 / T). \quad (24)$$

The ratio of nuclear Curie constants is equal to the ratio of numbers of spins per unit volume, N_Q and N_D , in the two groups. Let us define α^2 , the ratio of mean square effective local fields:

$$\alpha^2 = h_Q^2 / h_D^2. \quad (25)$$

Finally, writing $N_Q = n_0 C$ where C is the impurity concentration and n_0 is the number of Q spins per impurity, Eqs. (22), (23), and (24) may be combined using $N_Q / N_D = n_0 C / (1 - n_0 C)$ to give

$$f = \frac{[1 + (\alpha - 1)n_0 C][1 + (\frac{1}{4}\alpha - 1)n_0 C]}{[1 + (\alpha^2 - 1)n_0 C][1 - \frac{3}{4}n_0 C]}. \quad (26)$$

Equation (26) will be used to fit the data of Sec. IV for zinc in aluminum.

²⁰ R. T. Schumacher, Phys. Rev. **112**, 837 (1958).

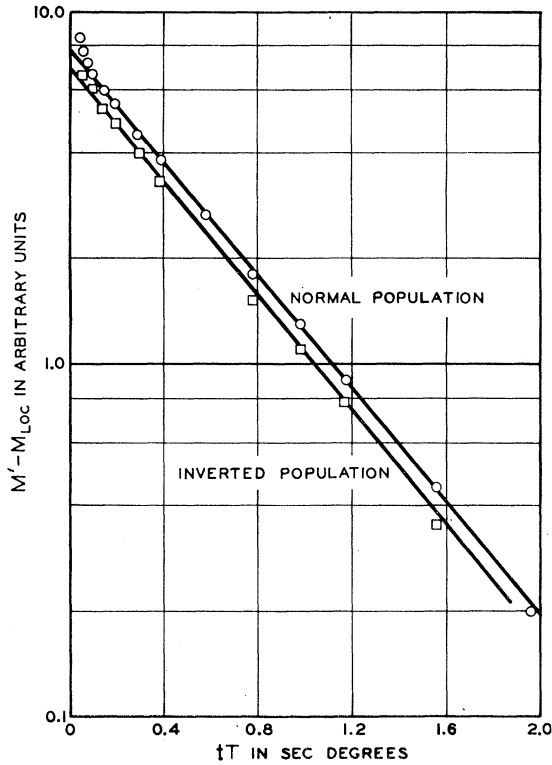


FIG. 2. Magnetization, $M' - M_{loc}$, vs tT for aluminum with 0.23 at. % of zinc showing relaxation for both normal (positive temperature) and inverted (negative temperature) initial spin distributions.

IV. ANALYSIS OF DATA

Figure 2 is a semilog plot of $(M' - M_{loc})$ vs tT for aluminum powder with 0.23 at. % of zinc; plotting against tT gives a universal plot for all temperatures. Zero-field relaxation is shown for both positive- and negative-temperature initial distribution. The sign of the negative-temperature curve was changed to make the plot. The two curves are very similar except for a scale factor and may be superimposed within experimental error. Thus, the relaxation seems to be the same for both types of distributions, in agreement with the predictions of spin temperature theories. There are at least two relaxation times present: The longer time is inversely proportional to temperature and is 0.36 sec at 1.5°K; the shorter time is independent of temperature in the liquid helium range. Thus, the shorter time fits the cross-relaxation time and the longer, temperature-dependent time is τ_1 ; in this case $\tau_1(0)/\tau_1$ is nearly $\frac{1}{3}$, indicating that the Q spins dominate the spin lattice relaxation for such an impurity concentration as the Q and D spins relax together.

Figure 3 is the plot of $(M' - M_{loc})$ vs t at 2.2°K for aluminum powder of ordinary impurity content (1.5 parts per thousand mostly of gallium). Again the curves show a fast, temperature-independent relaxation time and a slow time which is inversely proportional to

temperature. In this case insufficient rf field was used during adiabatic fast passage to turn over all of the nuclear magnetization. This is equivalent to inverting all of the spins to obtain a negative temperature and then heating them a little before demagnetizing. Under such circumstances the relaxation for the negative-temperature initial distribution should show the same type of relaxation as that for the positive-temperature distribution: The short and long relaxation times should be the same, but the relative amplitudes of the cross relaxation and τ_1 modes should differ in two cases. Figure 3 shows this to be the case.

Figure 4 is a plot of $(M' - M_{loc})$ vs tT for several concentrations of zinc in aluminum for positive-temperature relaxation in each case. All three curves start at $(M' - M_{loc}) = 10.0$ for $tT = 0$. The short and long times remain about the same as the concentration of zinc is increased, but the ratio and amplitude of the two relaxation modes change with zinc concentration. Effects can be noticed down to impurity concentrations of about one part in 10^{-4} . The curves have the form given in Appendix I; $\tau_1(0)/\tau_1 \approx 1/3$ indicating that the Q spins dominate the spin-lattice relaxation in all three cases.

After separating out the cross-relaxation part of the zero-field relaxation for each concentration of zinc impurity, the results shown in Table I were obtained. To fit the results using Eq. (26) for f , the fraction of cross-relaxation mode, versus impurity concentration, one needs n_0 , the number of Q spins per impurity, and α^2 , the ratio of h_Q^2 to h_D^2 , per Eqs. (25) and (26). As shown in Table I under calculated value, a good fit for f vs c can be obtained using Rowland's¹⁷ value of $n_0 = 98$ if we choose $\alpha = 3.75$, giving $\alpha^2 n_0 \approx 1400$. Un-

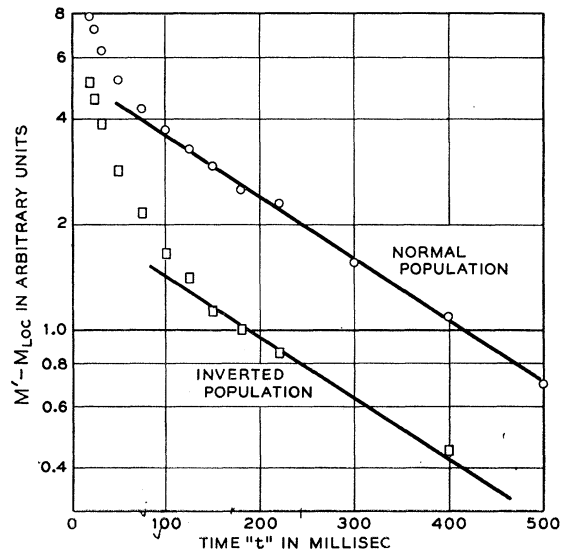


FIG. 3. Magnetization, $M' - M_{loc}$, vs time, t , for aluminum of ordinary impurity content showing relaxation for both normal (positive temperature) and inverted (negative temperature) initial spin distributions.

TABLE I. Values of f , the fractional signal remaining after a cycle for pure cross relaxation, vs C , the concentration of impurity. The calculated values are obtained from Eq. (26) as discussed in Sec. IV in the paragraphs concerning Fig. 4.

C in at. %	f (experimental)	f (calculated)
0.031	0.80 ± 0.04	0.79
0.075	0.65 ± 0.03	0.65
0.23	0.45 ± 0.03	0.49

fortunately, a full evaluation of α and n_0 can only be obtained with detailed knowledge of the quadrupolar splittings of aluminum nuclei near an impurity. However, an estimate has been made in Appendix II of $\alpha^2 n_0$ obtaining $\alpha^2 n_0 \approx 3500$. This agrees favorably with the result given above. The experimental value is somewhat low and may indicate that the innermost shell of the aluminum atoms near an impurity may not be fully participating in the cross-relaxation process which is seen. Another indication that the cross-relaxation time for this shell is longer appears in Fig. 4. The curve for the largest impurity concentration shows a $\tau_1(0)$ smaller than that of the other two concentrations; at increased concentration, such an additional relaxation mode could compete with τ_1 giving rise to the difference in the curves. At the highest concentration used, the impurity atoms are still spaced sufficiently far apart on the average that effects from overlap of quadrupole spin groups should be negligible.

Finally, Fig. 5 is a plot of $\tau_1 T$ vs field for two concentrations of zinc impurity; the values⁵ for a pure sample are close to those for the lowest impurity concentration. Equations (10) and (11), the result of the theory with dipolar coupling only,¹¹ show that

$$\tau_{1D}(H)T = \tau_1 T (H^2 + (5/3)\langle \Delta H^2 \rangle_{av}) / (H^2 + (10/3)\langle \Delta H^2 \rangle_{av}). \quad (27)$$

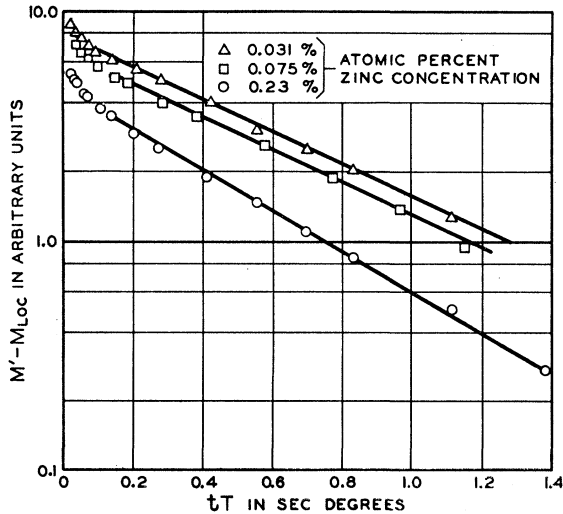


FIG. 4. Magnetization, $M' - M_{100}$, vs tT for aluminum of several concentrations of zinc impurity. All curves are for normal (positive temperature) relaxation and start at $(M' - M_{100}) = 10.0$ at $tT = 0$.

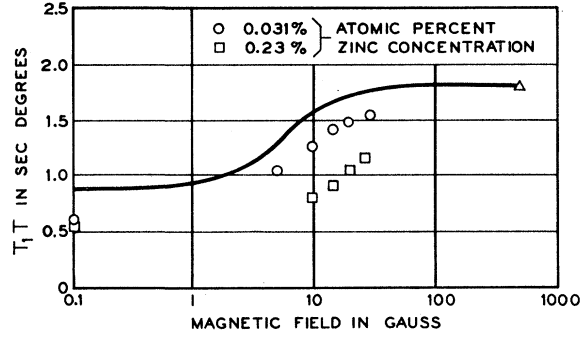


FIG. 5. $\tau_1 T$ vs magnetic field for aluminum with two concentrations of zinc impurity; the point labeled with a triangle is common to both concentrations of impurity. The curve is based on Eq. (27).

The curve in Fig. 5 is a plot of Eq. (27) using $\tau_1 T = 1.80$ sec°K and using $\langle \Delta H^2 \rangle_{av} = 9.8$ (G).²¹ The experimental data only qualitatively agree with the curve. First, the theory predicts $\tau_1(0)/\tau_1 = 1/2$, which is not found even in pure samples. Anderson and Redfield⁵ showed that $\tau_1(0)/\tau_1 = 1/2.2, 1/2.28, 1/2.58$, and $1/2.72$ for pure lithium, sodium, copper, and aluminum, respectively. Quadrupolar effects from impurities should have been negligible in their samples. They attributed the discrepancy to the effect of correlated relaxation of neighboring nuclear spins by conduction electrons, which reduces $\tau_1(0)$ relative to τ_1 . To obtain such a correlated relaxation the theory must be extended beyond the one-electron approximation. Preliminary calculation by Wolff²¹ shows that electron correlation effects are too small by a factor of 2 to explain the discrepancy in $\tau_1(0)/\tau_1$ for lithium and sodium, and they give much too small a correction for copper and aluminum as calculated with the random phase approximation. In addition, the “knee” of the curve in Fig. 5 is in the wrong place even in a pure sample. Thus, the spin-temperature approximation results in an error of a factor of 2 in the value of external field at which high-field (Zeeman) relaxation passes over to low-field (dipolar) relaxation. The shift in the knee of the curve in Fig. 5 for the sample of higher impurity concentration results from the need to use hQ^2 [with Eq. (15)] instead of hD^2 [with Eq. (27)]. In fact, one needs $hQ^2 > hD^2$ or $\alpha^2 > 1$; as previously noted, α^2 was estimated as 3.75. A detail calculation of the field dependence for such a case would be difficult since τ_{12} itself would be expected to depend on field.

V. CONCLUSIONS

The spin temperature of approximation works well in describing zero-field nuclear spin relaxation in metals provided strong impurity effects are taken into account. The relaxation curves are the same for both positive- and negative-temperature initial distribution, a situation predicted by a theory based on spin temperature but difficult to obtain otherwise. The data do not permit

²¹ P. Wolff (private communication).

resolution of more than two relaxation times. The cross-relaxation process between the Q spins and the D spins is adequately described by a model which allows each shell of quadrupole spins near an impurity to relax together with a single spin temperature. To do better and to properly consider the role of the "boundary" spins would require detailed knowledge of the quadrupole spin splittings, but the data hardly justify considering a more detailed cross relaxation. However, the spin-temperature approximation fails to predict the proper field dependence of τ_1 , indicating that the approximation may be poor in the transition region when the external field is of the order of the local field.

ACKNOWLEDGMENTS

The author wishes to thank several members of the Bell Telephone Laboratories for their help: J. Strautins for technical assistance; J. Wernick and R. F. Jack for help in sample preparation; J. K. Galt and P. Wolff for several discussions concerning the relaxation effects; and S. J. Buchsbaum for critical reading of the manuscript.

APPENDIX I

The time dependence of T_{SQ} and T_{SD} at zero field can be obtained in the spin-temperature approximation from equations developed by Schumacher²⁰ using the method of reference 4. He analyzed the relaxation of two coupled spin systems which relax to the lattice. The method will be outlined below as applied to the relaxation of spin temperatures of the Q and D systems at zero field. The method calculates the rate of change of spin energy, which is considered both as a function of spin temperature and as a function of the spin level populations. Using E_n^D and p_n to label the spin energy and population of the n th level of the D system, and using E_r^Q and q_r to label the spin energy and population of the r th level of the Q system, one may write

$$\begin{aligned} \frac{d}{dt}\bar{E}_D &= \frac{d}{dt}\bar{E}(T_{SD}) = \frac{\partial \bar{E}^D}{\partial T_{SD}} \frac{\partial T_{SD}}{\partial t} \\ &= -T_{SD}^2 \frac{\partial \bar{E}_D}{\partial T_{SD}} \frac{d}{dt} \left(\frac{1}{T_{SD}} \right) \quad (A1) \end{aligned}$$

$$= -\frac{d}{dt} \sum_n p_n E_n^D = \sum_n \frac{dp_n}{dt} E_n^D; \quad (A2)$$

also,

$$\begin{aligned} \frac{d}{dt}\bar{E}_Q &= \frac{d}{dt}\bar{E}(T_{SQ}) = \frac{\partial \bar{E}_Q}{\partial T_{SQ}} \frac{dT_{SQ}}{dt} \\ &= -T_{SQ}^2 \frac{\partial \bar{E}_Q}{\partial T_{SQ}} \frac{d}{dt} \left(\frac{1}{T_{SQ}} \right) \quad (A3) \end{aligned}$$

$$= -\frac{d}{dt} \sum_r q_r E_r^Q = \sum_r \frac{dq_r}{dt} E_r^Q. \quad (A4)$$

\bar{E}_D and \bar{E}_Q have already been evaluated in Eq. (18) in Sec. III. Noting that $\partial \bar{E}_D / \partial T_{SD}$ and $\partial \bar{E}_Q / \partial T_{SQ}$ are the spin specific heats at constant field, ζ_{HD} and ζ_{HQ} , one obtains

$$\frac{d}{dt} \left(\frac{1}{T_{SD}} \right) = -\frac{1}{T_{SD}^2 \zeta_{HD}} \sum_n E_n^D \frac{dp_n}{dt} \quad (A5)$$

and

$$\frac{d}{dt} \left(\frac{1}{T_{SQ}} \right) = -\frac{1}{T_{SQ}^2 \zeta_{HQ}} \sum_r E_r^Q \frac{dq_r}{dt}. \quad (A6)$$

For weak perturbations one can write rate equations for the population changes in terms of transition probabilities. There are two types of terms: The first involves W_{nm}^D (or W_{rs}^Q), the probability per unit time for a transition of the D system from state n to state m (or the Q system state r to state s), which is induced by the spin-lattice interaction, \mathcal{H}' , Eq. (5); the second type involves $W_{nr,ms}$, the probability per unit time for a transition of the D system from state n to state m with a transition of the Q system from state r to state s , which is induced by the cross-relaxation mechanism. In these terms

$$\begin{aligned} dp_n/dt &= \sum_m (p_m W_{mn} - p_n W_{nm}) \\ &\quad + \sum_{m,r,s} (p_m q_s W_{ms,nr} - p_n q_r W_{nr,ms}) \quad (A7) \end{aligned}$$

and

$$\begin{aligned} \frac{dq_r}{dt} &= \sum_s (q_s W_{sr} - q_r W_{rs}) \\ &\quad + \sum_{s,n,m} (p_m q_s W_{ms,nr} - p_n q_r W_{nr,ms}). \quad (A8) \end{aligned}$$

To guarantee equilibrium the principle of detail balance requires:

$$\frac{p_m W_{mn}}{p_n W_{nm}} = \exp \left[(E_n^D - E_m^D) \left(\frac{1}{kT_{SD}} - \frac{1}{kT} \right) \right], \quad (A9)$$

$$\frac{q_s W_{sr}}{q_r W_{rs}} = \exp \left[(E_r^Q - E_s^Q) \left(\frac{1}{kT_{SQ}} - \frac{1}{kT} \right) \right], \quad (A10)$$

and

$$\frac{p_m q_s W_{ms,nr}}{p_n q_r W_{nr,ms}} = \exp \left[(E_n^D - E_m^D) \left(\frac{1}{kT_{SD}} - \frac{1}{kT_{SQ}} \right) \right]. \quad (A11)$$

Equation (A11) can also be written in terms of E_r^Q and E_s^Q since $E_n^D - E_m^D = -(E_r^Q - E_s^Q)$ to conserve energy.

Substitution of Eqs. (A9), (A10), and (A11) into Eqs. (A7) and (A8) gives the rate of change of populations, to be substituted into Eqs. (A5) and (A6) to obtain the desired rate of change of spin temperatures. Now since both the D and Q spin splittings are small compared to T_{SD} , T_{SQ} and T , the exponentials in Eqs. (A9), (A10), and (A11) can be expanded and only the first-order terms kept. After some algebra one

finally obtains

$$\frac{d}{dt}\left(\frac{1}{T_{SD}}\right) = -\frac{1}{T_{1D}}\left(\frac{1}{T_{SD}} - \frac{1}{T}\right) - \frac{A}{\zeta_{HD}}\left(\frac{1}{T_{SD}} - \frac{1}{T_{SQ}}\right) \quad (\text{A12})$$

and

$$\frac{d}{dt}\left(\frac{1}{T_{SQ}}\right) = -\frac{1}{T_{1Q}}\left(\frac{1}{T_{SQ}} - \frac{1}{T}\right) + \frac{A}{\zeta_{HQ}}\left(\frac{1}{T_{SD}} - \frac{1}{T_{SQ}}\right). \quad (\text{A13})$$

The expressions for the spin-lattice relaxation time, τ_1 , for each system and for the cross-relaxation coupling term, A , are given in reference 20. The concern here is only with the time dependence of the solution, since lack of detailed knowledge of the levels of the Q system precludes effective use of the formal expression for A . By setting $\tau_{1D} = \tau_{1Q} = \infty$ and subtracting (A13) from (A12), one notes that the cross-relaxation time, τ_{12} , can be identified:

$$\frac{1}{\tau_{12}} = A\left(\frac{1}{\zeta_{HD}} + \frac{1}{\zeta_{HQ}}\right). \quad (\text{A14})$$

As anticipated in Sec. III, the Eqs. (A12) and (A13) can be easily solved with the aid of (A14) in the limit that $\tau_{12} \ll \tau_{1D}$ or τ_{1Q} . If, in addition, $\zeta_{HQ} \gg \zeta_{HD}$, so that the Q system dominates the relaxation, one obtains a simple solution:

$$\frac{1}{T_{SD}} \cong \frac{1}{T} + \left(\frac{1}{T_{SQ}(0)} - \frac{1}{T}\right) \exp(-t/\tau_{1Q}) + \left(\frac{1}{T_{SD}(0)} - \frac{1}{T_{SQ}(0)}\right) \exp(-t/\tau_{12})$$

and

$$\frac{1}{T_{SQ}} \cong \frac{1}{T} + \left(\frac{1}{T_{SQ}(0)} - \frac{1}{T}\right) \exp(-t/\tau_{1Q}). \quad (\text{A15})$$

In this limit, T_{SD} relaxes to T_{SQ} and then the two systems relax together toward the lattice temperature. If $\tau_{12} \ll \tau_{1D}$ or τ_{1Q} with no restriction on the ratio of ζ_{HQ} to ζ_{HD} , the solution is more complicated, but it still contains only two modes: the fast τ_{12} mode (as T_{SD} and T_{SQ} approach on another) and a "mixed" τ_1 mode, the mixture depending on the ratio of ζ_{HQ} to ζ_{HD} . Thus, the spin-temperature approximation provides the basis for the two-mode decay analysis used in Secs. III and IV.

APPENDIX II

Although the exact splittings of the spins in the Q system are not known, an estimate can be made of $\alpha^2 n_0$, where n_0 is the number of Q spins per impurity and α^2 is the ratio of mean square effective local fields for the Q and D spins. That is, from Eqs. (25), (11), and (16),

$$\alpha^2 n_0 = n_0 \frac{h_Q^2}{h_D^2} = n_0 \frac{\text{Tr}_Q \mathcal{H}_Q^2 \text{Tr}_D \mathcal{H}_D^2}{\text{Tr}_D \mathcal{H}_D^2 \text{Tr}_Q \mathcal{H}_Q^2}. \quad (\text{A16})$$

Using $\text{Tr}_Q \mathcal{H}_Q^2 = N \gamma^2 \hbar^2 [I(I+1)/3] (2I+1)^N$, one has

$$\alpha^2 n_0 = n_0 \left(\frac{N_D}{N_Q}\right) \frac{\text{Tr}_Q \mathcal{H}_Q^2}{(2I+1)^{N_Q}} \frac{(2I+1)^{N_D}}{\text{Tr}_D \mathcal{H}_D^2}. \quad (\text{A17})$$

Now \mathcal{H}_Q , Eq. (14), depends upon $eq(R_{ik})$, the electric field gradient of the i th solute nuclei at a distance R_{ik} from the k th impurity. It is given by Eq. (13).

$$eq(R_{ik}) = A \cos(2k_F R_{ik} + \varphi) / R_{ik}^3. \quad (\text{A18})$$

n_0 is the number of spins near an impurity for which the mean-square quadrupolar energy per spin is greater than the mean-square dipolar energy per spin. If we label each spin at the boundary of a Q region by b , then the mean-square quadrupolar energy of such a spin is given by

$$\langle E_{Qb^2} \rangle_{av} = \text{Tr}_b \mathcal{H}_Q^2 / (2I+1), \quad (\text{A19})$$

where $\mathcal{H}_Q = \sum_i \mathcal{H}_{Qi}$. The mean-square dipolar energy per spin is given by

$$\langle E_{Db^2} \rangle_{av} = \text{Tr}_D \mathcal{H}_D^2 / N_D (2I+1)^{N_D}. \quad (\text{A20})$$

Equating $\langle E_{Qb^2} \rangle_{av}$ and $\langle E_{Db^2} \rangle_{av}$ to determine the boundary, one finds

$$\frac{N_D (2I+1)^{N_D}}{\text{Tr}_D \mathcal{H}_D^2} = \frac{(2I+1)}{\text{Tr}_b \mathcal{H}_Q^2}. \quad (\text{A21})$$

Substituting from Eq. (A21) into Eq. (A17), one has

$$\alpha^2 n_0 = \left(\frac{n_0}{N_Q}\right) \frac{\text{Tr}_Q \mathcal{H}_Q^2}{(2I+1)^{N_Q} \text{Tr}_b \mathcal{H}_Q^2} = \left(\frac{n_0}{N_Q}\right) \frac{\sum_{i,k} q^2(R_{ik})}{q^2(R_{bk})}. \quad (\text{A22})$$

But n_0/N_Q is just the number of impurity atoms. Since the gradients are the same about each like impurity, the sum over k can be done in Eq. (A22) canceling n_0/N_Q . Dropping the label k on R_{bk} , one has

$$\alpha^2 n_0 = \frac{\sum_{i \in b} q^2(R_i)}{q^2(R_b)} = \frac{\sum_{i \in b} \cos^2(2k_F R_i + \varphi) / R_i^6}{\cos^2(2k_F R_b + \varphi) / R_b^6}. \quad (\text{A23})$$

Now R_b is directly related to n_0 itself. Since there are 18 atoms in the first two shells in a face-centered-cubic lattice, $n_0 \cong 18 R_b^3 / r_0^3$ where r_0 is the cube edge distance. Therefore,

$$\alpha^2 n_0 \cong \left(\frac{n_0}{18}\right)^2 \frac{\sum_{i \in b} \cos^2(2k_F R_i + \varphi) (r_0/R_i)^6}{\cos^2(2k_F R_b + \varphi)}.$$

The amplitude, A , of $eq(R_{ik})$ has dropped out in terms of n_0^2 . This is the virtue of considering the quantity $\alpha^2 n_0$. To go further and obtain an approximate value, $\cos^2(2k_F R_i + \varphi)$ is taken to be $\frac{1}{2}$. Further, the sum over i converges rapidly and there is little error in summing over all shells when $n_0=98$, the value found by Row-

land¹⁷ for zinc in aluminum. Since $\sum_i (r_0/R_i)^6 \cong 115$ for a face-centered cubic lattice, therefore,

$$\alpha^2 n_0 \cong (98/18)^2 \times 115 \cong 3500.$$

This value of $\alpha^2 n_0$ is compared in Part IV with the value deduced from experiment.

Effect of Pressure on the Energy Levels of Impurities in Semiconductors. I. Arsenic, Indium, and Aluminum in Silicon*

M. G. HOLLAND† AND WILLIAM PAUL

Division of Engineering and Applied Physics, Harvard University, Cambridge, Massachusetts

(Received May 21, 1962)

The changes in resistivity of silicon samples containing group III and group V impurities have been measured at hydrostatic pressures up to 6000 kg cm⁻² at 50°K. The changes are explained by a dependence on pressure of the ionization energy of the majority impurity center. The results indicate that the arsenic energy level moves toward the conduction-band edge at a rate of approximately 5×10^{-8} eV kg⁻¹ cm². The energy levels for indium and aluminum move away from the valence-band edge at rates of about 5×10^{-8} eV kg⁻¹ cm² and 1×10^{-8} eV kg⁻¹ cm², respectively. Corrections for the changes in mobility with pressure have been applied for the n -type sample. The motion of the arsenic energy level is explained by a change in dielectric constant and effective mass with pressure, and indicates a change in the average effective mass of less than 1% in 5000 kg cm⁻². The very small changes in ionization energy, while expected, are to be contrasted with the much larger changes found for the deep-lying levels produced by elements such as gold.

INTRODUCTION

THE effects of high hydrostatic pressure on the properties of a number of semiconductors can be understood using a model based on changes in the band structure of the materials.¹ For germanium and silicon, the pressure variation of the intrinsic resistivity,² the carrier mobilities,³ the magnetoresistance coefficients,⁴ the fundamental absorption edge,⁵ and the dielectric constant⁶ can be explained by the shift of the appropriate band edges with pressure. Since some of the most important properties of semiconductors are due to the presence of foreign atoms in the host lattice, the effect of pressure on the ionization energy of the electrons or holes on certain of these impurity

centers has been measured, with the hope that the present model can be used to explain the results.

The best understood impurity atoms in germanium and silicon are the so-called "hydrogenic" impurities, the group III and group V elements of the periodic table. The simple theory⁷ predicts that the impurity ionization energy will be given by

$$E = (e^2 m_{\text{eff}}) / (2a_h m_0 K^2), \quad (1)$$

where m_{eff} is the electron effective mass, m_0 the electron mass, K the dielectric constant, e the electronic charge, a_h the radius of the first Bohr orbit in hydrogen, and $e^2/2a_h = 13.62$ eV = the ionization energy of hydrogen. The quantum-mechanical treatment of Kohn and Luttinger⁸ also gives Eq. (1) for n -type silicon. For p -type silicon the approximations leading to Eq. (1) do not hold. Experimentally, the ionization energy can be related to the number of current carriers in the crystal. In general, the relation between the carrier density n and the impurity ionization energy E can be quite complex, but at low enough temperature we can write⁹

$$n = A \exp(-E/kT), \quad (2)$$

⁷ H. Brooks, *Advances in Electronics and Electron Physics*, edited by L. Marton (Academic Press Inc., New York, 1955), Vol. 7, p. 102.

⁸ See W. Kohn, *Solid State Physics*, edited by F. Seitz and D. Turnbull (Academic Press Inc., New York, 1957), Vol. 5, p. 280.

⁹ See reference 7, p. 124.

* Supported by the Office of Naval Research. The article is based on a thesis presented to Harvard University by M. G. Holland in partial fulfillment of the requirements for the Ph.D. degree, May, 1958.

† Present address: Research Division, Raytheon Company, Waltham, Massachusetts.

¹ W. Paul, *J. Phys. Chem. Solids*, **8**, 196 (1959) (and references quoted therein).

² W. Paul and H. Brooks, *Phys. Rev.* **94**, 1128 (1954); W. Paul and G. L. Pearson, *ibid.* **98**, 1755 (1955).

³ A. C. Smith, *Bull. Am. Phys. Soc.* **3**, 14 (1958); A. C. Smith, Technical Report H. P. 2, Gordon McKay Laboratory, Harvard University, 1958 (unpublished).

⁴ G. B. Benedek, W. Paul, and H. Brooks, *Phys. Rev.* **100**, 1129 (1955).

⁵ W. Paul and D. M. Warschauer, *J. Phys. Chem. Solids*, **5**, 89, 102 (1958); **6**, 6 (1958).

⁶ M. Cardona, W. Paul, and H. Brooks, *J. Phys. Chem. Solids*, **8**, 204 (1959).